

IMPROVING THE EFFICIENCY OF HEAT RECOVERY CIRCUITS OF COGENERATION PLANTS WITH COMBUSTION OF WATER-FUEL EMULSIONS

by

**Victoria KORNIENKO^{a*}, Mykola RADCHENKO^b, Roman RADCHENKO^b,
Dmytro KONOVALOV^a, Andrii ANDREEV^a, and Maxim PYRYSUNKO^a**

^a Admiral Makarov National University of Shipbuilding (Kherson branch), Kherson, Ukraine

^b Admiral Makarov National University of Shipbuilding, Mykolaiv, Ukraine

Original scientific paper

<https://doi.org/10.2298/TSCI200116154K>

When using modern highly efficient internal combustion engines with lowered potential of exhaust heat the heat recovery systems receive increasing attention. The efficiency of combustion exhaust heat recovery at the low potential level can be enhanced by deep cooling the combustion products below a dew point temperature, which is practically the only possibility for reducing the temperature of boiler exhaust gas, while ensuring the reliability, environmental friendliness and economy of power plant. The aim of research is to investigate the influence of multiplicity of circulation and temperature difference at the exit of exhaust gas boiler heating surfaces, which values are varying as 20 °C, 15 °C, and 10 °C on exhaust gas boiler characteristics. The calculations were performed to compare the constructive and thermal characteristics of the various waste heat recovery circuits and exhaust gas boiler of ship power plant. Their results showed that due to application of condensing heating surfaces in exhaust gas boiler the total heat capacity and steam capacity of exhaust gas boiler increases. The increase of exhaust gas boiler heat capacity is proportional to the growth of its overall dimensions. A direct-flow design of the boiler provides a significant increase in heat efficiency and decrease in dimensions. In addition, a direct-flow boiler circuit does not need steam separator, circulation pump, the capital cost of which is about half (or even more) of heating surface cost.

Key words: *exhaust gas boiler, internal combustion engines, afterburning*

Introduction

With lowering the potential of heat losses in modern highly efficient internal combustion engines (ICE) the heat recovery systems receive increasing attention [1, 2]. Using the exhaust gas heat of ICE for production of low pressure steam in exhaust gas boiler (EGB) is the most simple way to utilize it. On ships with an ICE power of more than 15000 kW, due to relatively small steam needs only part of the exhaust gas heat of the main ICE is used in EGB, and therefore the heat recovery efficiency is relatively small. For a more full use of the exhaust gas heat of the ICE, more complex heat recovery circuit (HRC) schemes are used, and first of all, schemes with recovery turbogenerators (RTG). When the RTG is incorporated into the ship power plant (SPP), the maneuverability of the SPP significantly enhanced. The main issues of

* Corresponding author, e-mail: kornienkovika1987@gmail.com

additional electricity generation through the recovery of combustion products heat are production of small turbines and the assessment of economic feasibility of creating such plants.

A depth of utilizing the heat of engine exhaust gas influences considerably on the efficiency of any thermal power plant from cogenerative ICE [3] and gas turbines [4] to trigenerative plants generating heat [5], electricity power [6] and cooling [7] (refrigeration and air conditioning), *i.e.* practically in all waste heat recovery technics [8, 9]. Different methods of modeling [10, 11] and optimization [12] of such heat recovery technics are used.

The efficiency of combustion heat recovery can be enhanced by deep cooling the combustion products below the dew point temperature, which is practically the only possibility of reducing the exhaust gas temperature of EGB while ensuring the reliability, environmental friendliness and economy of SPP. Sharp increasing the low temperature corrosion (LTC) rate (up to 1.5 mm per year at wall temperatures below 130 °C with the combustion of sulfur fuels with water content $W^r = 2\%$), decreasing of EGB steam capacity and depth of gas heat recovery has taken place. Therefore, decreasing of LTC intensity at the surface temperature below a dew point temperature of sulfuric acid vapor H_2SO_4 is practically the only possibility of reducing the EGB exhaust gas temperature.

The results of studies [13, 14] showed that when water-fuel emulsions (WFE) are combusted with a water content W^r of 30% and excess air factor $\alpha = 1.05-1.45$, the LTC velocity level is below the permissible level of 0.2 mm per year, which allows to install the condensing heating surfaces in auxiliary boiler and thereby to increase the utilization depth.

Literature review

The experience of application of WFE in boilers and engines indicates the advantages of this type of fuel [15, 16]. At maximum power modes in the exhaust gases the concentration of NO_x is significantly reduced by 1.3-3.5 times, the concentration of CO – by 1.3-2 times, the smoke – by 1.6-2.5 times, and SO_x decreases by 1.8 times [17, 18].

The CIMAC 2007 report describes a 6 MW cogeneration unit with gas engines that simultaneously produce heat and electricity, which is equipped with a turbocompound system, which includes a combustion chamber in front of the turbine with additional fuel and air. Such an installation, with the same amount of steam that is produced, provides a high overall (heat and electricity) efficiency of the installation 70-80% depending on the load, high efficiency of electricity generation (38%) and a shorter payback period (3-4 years) compared to medium and small sized gas turbines (their parameters are in accordance with 55-73%, 28-30% and 6-8 years).

The exhaust gas heat can be recovered by absorption heat pump for district heating [19, 20]. Li *et al.* [19] introduced the technique of exhaust gas heat utilization in gas cogeneration unit by absorption heat exchange. The heat exchangers used to heat water are called low temperature economizers or low pressure economizers [21]. Wang *et al.* [22] and Fan *et al.* [23] analyzed the energy saving effects of low pressure economizer applied on coal-fired units. According to data of [24, 25] the installation of low temperature and low pressure improved the energy saving effect of units.

Nevertheless, the wall temperature of heating surface of EGB and exhaust gases must be no lower than dew point temperature of sulfuric acid vapor in exhaust gas. Because, the acid vapor are condensed on the heating surface, and corrode exhaust heat economizers, which will shorten their life [13, 14].

The aim of research is to investigate the influence multiplicity of circulation and the value of temperature head over the heating surfaces, Δt , which were taken at the level of

20 °C, 15 °C, 10 °C, on EGB characteristics. The research task is to obtain experimental data of corrosion intensity of EGB heating surfaces on using WFE afterburning with water content 30% and excess air factor α from 1.5 to 2.5.

Research Methodology

The investigations of corrosion processes development were carried out at the experimental installation. On the experimental set-up, fig. 1, the series of 25 experiments were conducted with the combustion of various standard fuels (DF, M40, M100) during time τ from 2 to 12 hours; at a sulfur content, S^r , in fuels from 0.7% to 2%; at excess air factor, α , from 1.01 to 1.5; water content of 2%, as well as WFE based on M40 with water content from 4 to 30%, at α from 2.15 to 2.5.

The WFE preparation for combustion in experimental set-up was carried out in special installation. The experimental installation includes the following elements: combustion chamber, burner, fuel preparation system, gas pipeline. For experimental research, special probes with tube samples were made. The assemblies of the three tube samples were installed in the gas pipeline of the experimental set-up at gas velocity of 7-8 m/s. The tube samples were cooled by water or oil. Determination of corrosion intensity external surface of tube samples was carried out by gravitation method.

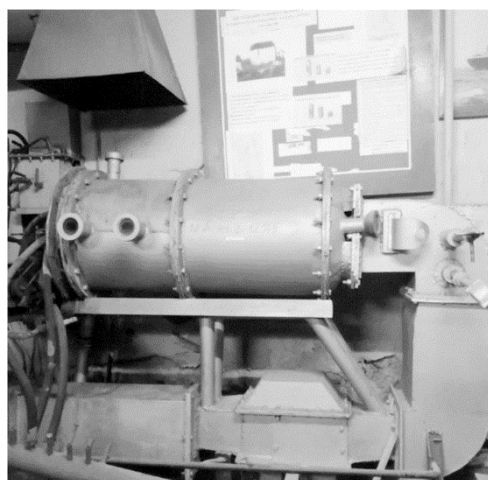


Figure 1. Drawing of experimental set-up

The temperature of exhaust gases and tube samples were measured by thermocouples, which were on tube samples and in spaces between the tubes. Analysis of exhaust gas composition at the furnace outlet is carried out by a chemical gas analyzer (determination of RO_2 and O_2), a chromatograph (determination of CO , H_2 , and CH_4), gas analyzers (determination of SO_x and NO_x). Determination of corrosion speed of metal surface, K , of tube samples due to LTC was carried out by the gravitation method. The determination of masses were performed by using laboratory weights.

Experiments were carried out with measurements of the geometric characteristics of each tube sample (the mean value of the diameter for two transverse measurements and its value), which made it possible to determine the outer area of the tube sample, F , for the test. After that we weighed each tube sample (before the experiment) – mass m_1 , fig. 2.

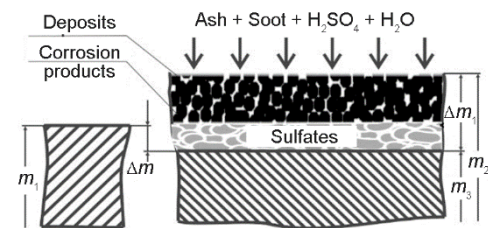


Figure 2. Drawing of corrosion processes investigation

At the end of experiment, packs of tube samples were pulled out from gas pipeline. Tube samples with corrosion products, acid and soot deposits were weighed again by analytical weights (mass m_2). Soot deposits and corrosion products from the metal surface were removed by treatment of tube samples in a 5% solution of hydrochloric acid, an inhibited by

urotropin (1 g per 1 L of solution). Then the tube samples were washed in water and gas, dried and weighed for the second time (mass m_3).

The K at a certain temperature of the tube wall was determined:

$$K = \frac{m_1 - m_3}{F\tau} = \frac{\Delta m}{F\tau} \quad (1)$$

When the probable error of measurements and the accuracy of experiments were determined, the methodology for determining the error of measurements of the corrosion rate used in the first published works on the corrosion rate during the burning of sulfur fuels was taken into account. Since the corrosion rate was determined by eq. (2), the relative error of determining the corrosion rate will be equal to:

$$\frac{\Delta K}{K} = \pm \left[\frac{\Delta(\Delta m)}{\Delta m} + \frac{\Delta F}{F} \right] \quad (2)$$

The relative error in measuring the area of the tube sample, in turn, is:

$$\frac{\Delta F}{F} = \frac{\Delta d}{d} + \frac{\Delta L}{L} \quad (3)$$

Weighing of the tube samples was carried out with an accuracy of 0.0001 g. For determining Δm , it is necessary to weigh the tube sample twice (before and after the experiment). The absolute error in determining the mass loss of the tube sample was 0.0002 g. Therefore, the relative error in determining Δm with a minimum mass loss of 0.04 g will be 0.5%.

The outer and inner diameters of the tube samples were measured with a micrometer in two mutually perpendicular planes with an accuracy of 0.01 mm. The length of the tube sample was measured using a caliper with an accuracy of 0.05 mm. The minimum internal diameter of the tube sample was 20 mm, the minimum length was 23 mm. The deviation from the average diameter in the measured sections was 0.22 mm. The relative error in determining the area of the corroding surface of the tube sample will be 1.18%. The total relative error in determining the corrosion rate will be 1.68%.

In those cases, when the number of tube samples at the temperatures differing by 1 °C to 2 °C for one combustion mode was more than three, it becomes possible to determine the probable error of this series of experiments. In studies of the kinetics of corrosion processes, the duration of the experiments is hours. Therefore, the systematic error in determining the corrosion rate was defined by:

$$\Delta K = \sqrt{\left(\frac{\Delta m}{\tau F}\right)^2 + \left(\frac{\Delta m}{\tau^2 F} \Delta \tau\right)^2 + \left(\frac{\Delta m}{\tau F^2} \Delta F\right)^2} \quad (4)$$

The error in determining the area of the tube sample was defined by:

$$\Delta F = \sqrt{\left(\frac{\partial F}{\partial d_{\text{ex}}}\Delta d\right)^2 + \left(\frac{\partial F}{\partial d_{\text{av}}}\Delta d\right)^2 + \left(\frac{\partial F}{\partial l}\Delta L\right)^2} \quad (5)$$

When the geometric dimensions of the tube sample were $d_{ex} = 25$ mm, $L = 23$ mm, the accuracy of measuring the diameter of the sample was 0.01 mm, and the length of the sample was 0.05 mm, the value was $\Delta F = 4.05 \cdot 10^{-6}$ m². The surface of the tube sample was $F = 0.001805$ m².

When corrosion tests are conducted, the limiting relative systematic error in determining the corrosion rate was assumed to be 10%. With this the corrosion rate, K , at each experiment time are at the level of $10 \Delta K$.

Calculation studies and comparisons of the efficiency of different recovery schemes were performed for SPP, in which engine 16V32 WARTSILA NSD corporation was rated as a ICE at a rated power of 9280 kW with a specific fuel consumption of 0.195 gk/Wh and an exhaust gas temperature of 350 °C.

In order to compare the constructive and thermotechnical characteristics of the various HRC and the EGB structures using the computer based on latest literature data, the thermal calculations of the various SPP HRC were performed, figs. 3 and 4.

The software makes it possible to calculate the thermal balances of HRC of two pressures of different layouts (including with the fuel afterburning in front of EGB).

In the study, the options were considered: obtaining only saturated steam in the EGB (without a superheater) and when part or all steam is sent through the superheater to RTG for obtaining the appropriate capacity while providing all consumers with steam.

Thermal calculations of two pressure EGB with installation of heating surface packets with forced multiple forced circulation and heating surfaces for hot water system (when WFE afterburning) with heating of feed water to EGB up to 120 °C in water heaters installed in charge air cooler, and at the water temperature at the inlet to hot water section at 70 °C, which became possible with the decrease of LTC intensity when WFE combustion. To find out the benefits of direct-flow EGB, their calculations were performed without feed water preheating.

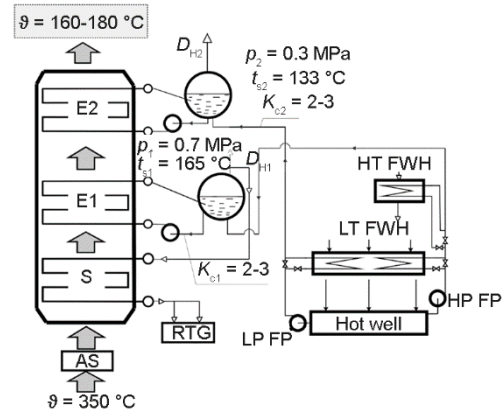


Figure 3. Thermal scheme of HRC of SPP with fuel oil combustion; S – high pressure superheater, E1, E2 – high and low pressure evaporator, HP FP, LP FP – high and low pressure feed pump, HT FWP, LT FWP – high and low temperature feed water heater, AS – afterburning system

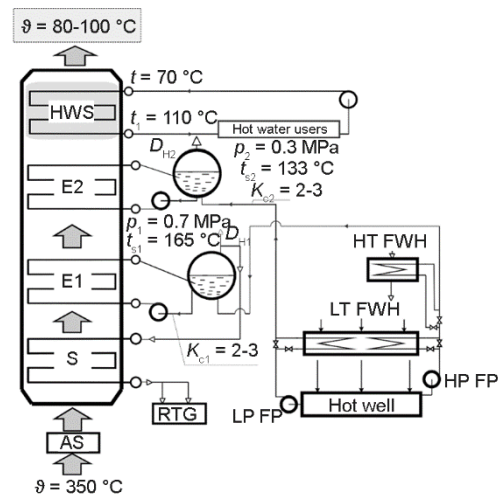


Figure 4. Thermal scheme of HRC of SPP with WFE afterburning; S – high pressure superheater, E1, E2 – high and low pressure evaporator, HWS – hot water section (condensing heating surface), HP FP, LP FP – high and low pressure feed pump, HT FWP, LT FWP – high and low temperature feed water heater, AS – afterburning system

The influence on the overall characteristics of EGB multiplicity of circulation and the values of the temperature pressure over the heating surfaces, Δt , which were taken at the level of 20 °C, 15 °C, and 10 °C, were conducted. Comparative studies of the overall characteristics of EGB heating surfaces were performed under the condition of same aerodynamic resistance of EGB ($\Delta h = \text{constant}$) at a constant gas velocity of ($w_g = \text{constant}$), which provides the same intensity of convective heat exchange in EGB heating surfaces. For ensuring the conditions $w_g = \text{constant}$ for $\Delta h = \text{constant}$, the width of pipeline, b , was changed at a constant length $l = \text{constant}$.

Energy efficiency of EGB depends on utilization depth K_u and are determined:

$$q_v = \frac{Q}{V\Delta t} \quad (6)$$

$$\Pi_v = K_u q_v \quad (7)$$

Results of investigation

Based on experimental research data, approximation equations of corrosion kinetic in the form dependences $K = f(t_w)$ were obtained, fig. 5.

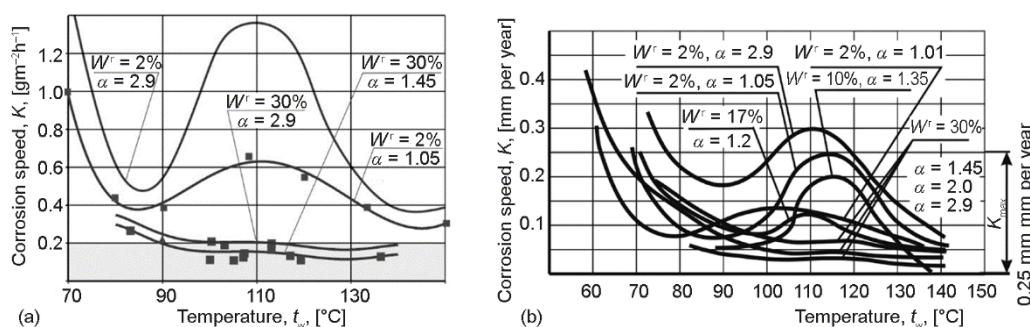


Figure 5. Correlation of corrosion intensity K from wall temperature

The dependences fig. 5(a) showed that LTC intensity is below the permissible level of 0.25 mm per year during afterburning of additional fuel in the form of WFE with water content of 30% and excess air factor $\alpha = 1.5$ -2.5 before EGB for 100 hours.

Figure 5(b) presents the results of studies, predicted at $\tau = 1000$ hours while ensuring constant combustion conditions and constant wall temperatures. These dependences make it possible to determine the minimum wall temperature of the low temperature surface according to the corrosion rate accepted under the conditions of reliability and service life.

Considering the permissible corrosion rate of the metal of the economizer at the level of 0.25-0.35 mm per year, it can be argued that the most dangerous level of LTC is the wall temperature range $t_w = 85$ -130 °C, because this part of the surface is subjected to intense exposure to sulfuric acid condensate. In this range of wall temperatures, the *acid peak* of corrosion is observed and the corrosion rate is well above the allowable level.

When WFE was burnt with different water content W^r varying from 4 to 17% a gradual decrease in the value of *corrosion peak* is observed. If at $W^r = 4\%$ the maximum value of the corrosion rate was 0.5 mm per year, then the WFE combustion with $W^r = 10\%$ – $K_{\text{max}} = 0.4$ mm per year, at $W^r = 17\%$ – $K_{\text{max}} = 0.25$ mm per year. The presence of a small

corrosion peak is observed. When WFE was burnt with water content 30%, there is no corrosion peak. Within the wall temperature varying from 140 °C to 70 °C, the corrosion rate is at the level of 0.15-0.3 mm per year. As a result, the corrosion intensity during the WFE combustion is reduced by six times compared to fuel combustion with $W^r = 2\%$. The service life of the heating surfaces increases proportionally. This means that, when WFE were burnt, the lifetime of the low temperature heating surface is the same as that of the dry one.

Obtained at the same electrical and thermal load values of fuel consumption showed that fuel consumption of SPP is reduced by 12% when WFE afterburning in front of EGB is used. The analysis of performed calculations indicates the feasibility of using WFE afterburning in the two pressure EGB, which depends primarily on the economics of ICE and the exhaust gas temperature.

The thermal diagram, fig. 6(a), shows that, while providing the accepted values of Δt , it is not possible to remove all the heat by using the economizer and vapor surfaces, since the heat dissipation is limited by the saturation temperatures, t_s , and by the value of temperature difference, Δt , between the temperature of exhaust gases and water or steam.

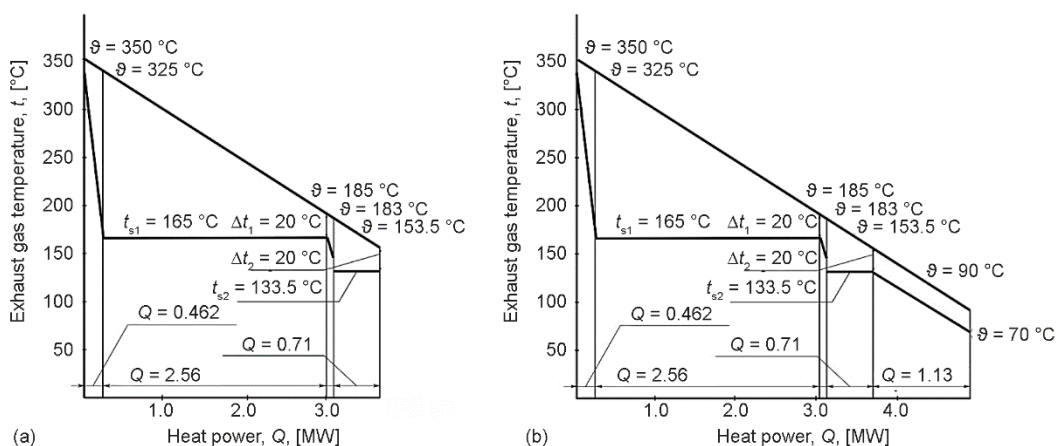


Figure 6. Thermal diagrams of different schemes of EGB; (a) two pressure EGB and (b) two pressure EGB with hot water section (condensing heating surface)

For ensuring deeper disposal, a hot water section must be installed (even if the feedwater temperature is 70 °C). In this case, the minimum value of exhaust gas temperature is due to the minimum surface heating temperature t_w and Δt_{\min} . The minimum value of t_w depends on the LTC intensity, the value of which decreases with WFE afterburning.

The calculations of thermal diagrams of EGB circuits, fig. 6(b) shows that due to the possibility of reducing the values of exhaust gas temperature from 160 °C to 90 °C using WFE afterburning with water content 30%, heat powers increase by 23%. In these schemes, the thermal characteristics of superheater (Q, D) are assumed constant.

Thermal calculations showed that installation of condensing heating surfaces in EGB increases the total capacity and steam capacity of EGB. The increase of EGB power is proportional to the growth of its overall indicators, fig. 7.

Reducing the temperature difference between the heating surface temperature and the gas temperature beyond the surface Δt leads to an increase in heat output, an increase in the required heating surface area H , volume V , and height h , figs. 8 and 9.

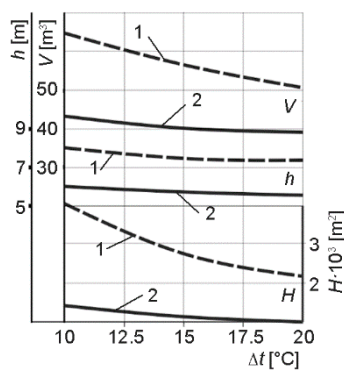


Figure 7. Dependence of volume, height, and surface area on Δt ; 1 – SPP with fuel oil combustion, 2 – SPP with WFE afterburning

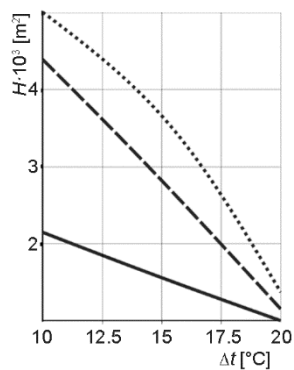


Figure 8. Dependence of surface area different schemes of EGB on Δt ; 1 – boiler with multiple forced circulation (counter current), 2 – boiler with multiple forced circulation (direct flow), 3 – direct-flow boiler

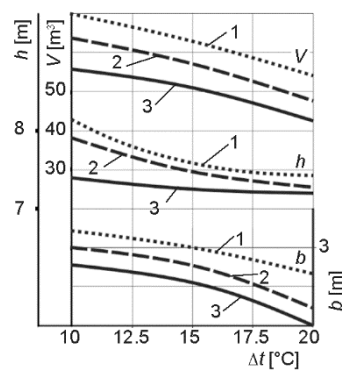


Figure 9. Dependence of volume, height, and width different schemes of EGB on Δt ; 1 – boiler with multiple forced circulation (counter current), 2 – boiler with multiple forced circulation (direct flow), 3 – direct-flow boiler

The smallest values of overall dimensions correspond to the direct-flow boiler. In addition, the direct-flow boiler circuit does not have steam separators, circulation pumps, the capital cost of which is half (or more) of heating surfaces cost.

The presented dependencies show that these metrics vary in different ways. Therefore, it is only important to compare the relative indicators, especially taking into account the utilization efficiency, overall indicators and values of Δt , as well as energy efficiency, figs. 10 and 11.

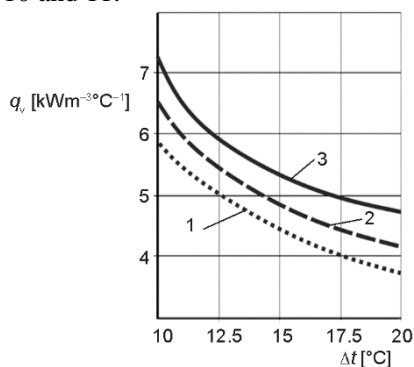


Figure 10. Dependence of the q_v values different schemes of EGB on Δt ; 1 – boiler with multiple forced circulation (counter current), 2 – boiler with multiple forced circulation (direct flow), 3 – direct-flow boiler

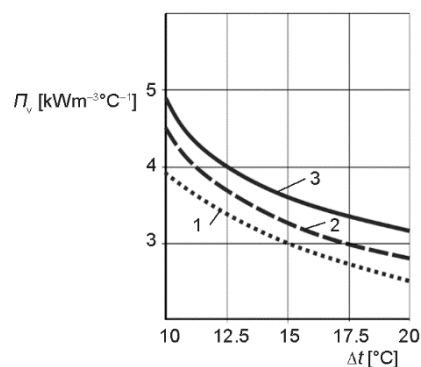


Figure 11. Dependence of the Π_v values different schemes of EGB on Δt ; 1 – boiler with multiple forced circulation (counter current), 2 – boiler with multiple forced circulation (direct flow), 3 – direct-flow boiler

These dependencies show that a significant increase in efficiency and an increase in overall dimensions is the case for a direct-flow boiler at $\Delta t = 10$ °C.

Conclusions

When using modern highly efficient ICE, despite the reduction in heat loss, heat recovery systems are receiving increasing attention. The efficiency of combustion exhaust heat recovery can be enhanced by deep cooling the combustion products below the dew point temperature, which is practically the only possibility of reducing the exhaust gas temperature of EGB while ensuring the reliability, environmental friendliness and economy of SPP.

The afterburning of additional fuel in the form of WFE with water content of 30% before EGB allows to provide the necessary conditions for passivation of EGB surface and reduction of LTC intensity up to 0.25 mm per year. On using WFE afterburning with water content 30% the heat capacity of EGB increases by 23% due to reducing the values of exhaust gas temperature from 160 °C to 90 °C.

The calculations were performed to compare the constructive and thermal characteristics of the various HRC and EGB. Due to application of condensing heating surfaces in EGB the total heat capacity and steam capacity of EGB increases. The increase of EGB heat capacity is proportional to the growth of its overall dimensions. A direct-flow design of the boiler provides a significant increase in heat efficiency and decrease in dimensions. In addition, a direct-flow boiler circuit does not need steam separator, circulation pump, the capital cost of which is about half (or even more) of heating surface cost.

Nomenclature

b – width of EGB, [mm]	Q – heat power, [MW]
d_{in} – internal diameter of the tube sample, [mm]	q_v – specific heat power, [kWm ⁻³ °C ⁻¹]
d_{ex} – external diameter of the tube sample, [mm]	Δt – temperature difference between the heating surface temperature and the gas temperature beyond the surface, [°C]
d_{av} – average diameter of the tube sample, [mm]	t_s – saturation temperature, [°C]
F – average surface of the outer surface of the tube sample to the experiment, [m ²]	t_w – wall temperature of heating surface, [°C]
H – heating surface area of EGB, [m ²]	V – volume of EGB, [m ³]
h – height of EGB, [m]	w_g – constant gas velocity, [ms ⁻¹]
Δh – aerodynamic resistance of EGB, [Pa]	W^r – water content of WFE, [%]
K – corrosion speed of metal surface, [gm ⁻² h ⁻¹]	<i>Greek symbols</i>
K_u – utilization depth, [-]	α – excess air factor
L – tube sample length, [mm]	Π_v – generalized performance indicator, [kWm ⁻³ °C ⁻¹]
Δm – mass loss of metal, [g]	τ – duration of experiment, [h]
m_1 – mass of tube sample before experiment, [g]	
m_3 – mass of tube sample after cleaning of soot deposits and corrosion products, [g]	

References

- [1] Radchenko, R., et al., Enhancing the Efficiency of Marine Diesel Engine by Deep Waste Heat Recovery on the Base of Its Simulation Along the Route Line, in: *Advances in Intelligent Systems and Computing*, (eds. Nechyporuk M. et al.), Integrated Computer Technologies in Mechanical Engineering, ICTM 2019, Springer, New York, USA, 2020, Vol. 1113, pp. 337-350
- [2] Bianco V., et al., Implementation of a Cogeneration Plant for a Food Processing Facility, A case study, *Applied Thermal Engineering*, 102 (2016), June, pp. 500-512
- [3] Possidente, R., et al., Experimental Analysis of Micro-Cogeneration Units Based on Reciprocating Internal Combustion Engine, *Energy and Buildings*, 38 (2006), 12, pp. 1417-1422
- [4] Yang, Ch., et al., Analytical Method for Evaluation of Gas Turbine Inlet Air Cooling in Combined Cycle power plant, *Applied Energy*, 86 (2009), 6, pp. 848-856
- [5] Li, H., et al., Influence of Fin Thickness on Heat Transfer and Flow Performance of a Parallel Flow Evaporator, *Thermal Science*, 23 (2019), 4, pp. 2413-2419

- [6] Radchenko A., et al., Increasing Electrical Power Output and Fuel Efficiency of Gas Engines in Integrated Energy System by Absorption Chiller Scavenge Air Cooling on the Base of Monitoring Data Treatment, *Proceedings, HTRSE-2018, E3S Web of Conferences* 70, 03011, 2018
- [7] Radchenko, M., et al., Enhancing the Utilization of Gas Engine Module Exhaust Heat by Two-Stage Chillers for Combined Electricity, Heat and Refrigeration, *Proceedings, 5th International Conference on Systems and Informatics, ICSAI 2018, Jiangsu, Nanjing, China, 2019*, pp. 240-244
- [8] Kumar, Tiwari A., et al., Effect of Ambient Temperature on the Performance of a Combined Cycle Power Plant, *Transactions of the Canadian Society for Mechanical Engineering*, 37 (2013), 4, pp. 1177-1188
- [9] Gunnur, Sen G., et al., The Effect of Ambient Temperature on Electric Power Generation in Natural Gas Combined Cycle Power Plant-A Case Study, *Energy Reports*, 4 (2018), Nov., pp. 682-690
- [10] Kuyumcu, M. E., et al., Thermal Analysis and Modeling of a Swimming Pool Heating System by Utilizing Waste Energy Rejected from a Chiller Unit of an Ice Rink, *Thermal Science*, 21 (2017), 6A, pp. 2661-2672
- [11] Volintiru, O. N., et al., Modeling and Optimization of HVAC System for Special Ships, *Journal of Physics: Conference Series*, 1122 (2018), 1, 012004
- [12] Volintiru, O. N., et al., Optimization of the Ventilation System for Special Ships, *Journal of Physics: Conference Series*, 1122 (2018), 1, 012034
- [13] Radchenko, M., et al., Semi-Empirical Correlations of Pollution Processes on the Condensation Surfaces of Exhaust Gas Boilers with Water-Fuel Emulsion Combustion, in: *Advances in Design, Simulation and Manufacturing II* (eds. Ivanov V. et al.), Lecture Notes in Mechanical Engineering, DSMIE 2019, Springer, New York, USA, 2020, pp. 853-862
- [14] Kornienko, V., et al., Correlations for Pollution on Condensing Surfaces of Exhaust Gas Boilers with Water-Fuel Emulsion Combustion, in: *Lecture Notes in Mechanical Engineering*, (eds. Tonkonogyi V. et al.), Grabchenko's International Conference on Advanced Manufacturing Processes, InterPartner-2019, Springer, New York, USA, 2020, pp. 530-539
- [15] Antonov, D., Strizhak, P. A., Explosive Disintegration of Two-Component Droplets in a Gas Flow at its Turbulization, *Thermal Science*, 23 (2019), 5B, pp. 2989-2993
- [16] Glushkov, D. O., et al., Rheological Properties of Coal Water Slurries Containing Petrochemicals, *Thermal Science*, 23 (2019), 5B, pp. 2939-2949
- [17] Patel, K. R., Dhiman, V., Research Study of Water - Diesel Emulsion as Alternative Fuel in Diesel Engine – An Overview, *International Journal of Latest Engineering Research and Applications*, 2 (2017), 9, pp. 37-41
- [18] Kruczynski, P., et al., Analysis of Selected Toxic Components in the Exhaust Gases of a CI Engine Supplied with Water-Fuel Emulsion, *Polish Journal of Environmental Studies*, 27 (2018), 1, pp. 129-136
- [19] Li, F., et al., Research and Application of Flue Gas Waste Heat Recovery in Cogeneration Based on Absorption Heat-Exchange, *Procedia Eng.*, 146 (2016), Dec., pp. 594-603
- [20] Wei, M., et al., Simulation of a Heat Pump System for Total Heat Recovery from Flue Gas, *Appl. Therm. Eng.*, 86 (2015), July, pp. 326-332
- [21] Jiayou, L., Fengzhong, S., Experimental Study on Operation Regulation of a Coupled High-Low Energy Flue Gas Waste Heat Recovery System Based on Exhaust Gas Temperature Control, *Energies*, 12 (2019), 4, 706
- [22] Wang, C., et al., Thermodynamic Analysis of a Low-Pressure Economizer Based Waste Heat Recovery System for a Coal-Fired Power Plant, *Energy*, 65 (2014), Feb., pp. 80-90
- [23] Fan, C., et al., A Novel Cascade Energy Utilization to Improve Efficiency of Double Reheat Cycle, *Energy Convers. Manag.*, 171 (2018), Sept., pp. 1388-1396
- [24] Huang, S., et al., An Improved System for Utilizing Low-Temperature Waste Heat of Flue Gas From Coal-Fired Power Plants, *Entropy*, 19 (2017), 423, pp. 1-17
- [25] Chen, H., et al., Field Study on the Corrosion and Ash Deposition of Low-Temperature Heating Surface in a Large-Scale Coal-Fired Power Plant, *Fuel*, 208 (2017), Nov., pp. 149-159